Scientia Iranica, Vol. 14, No. 5, pp 405–413

SCIENTIA IRANICA

Strengthening Design Limitations of an RC Frames Using FRP Column Wrapping Considering Column-to-Beam Strength Ratio

A.R. Khaloo* and A. Esmaili[1]

The aim of this paper is to study the influence of the column-to-beam strength ratio on the seismic strengthening of a column with a Fiber-Reinforced Plastic (FRP) wrapping system. FRP wrapped Reinforced Concrete (RC) columns are analyzed to obtain moment-curvature curves using FRP confined concrete characteristics. A pushover analysis of a 2D model was performed on one and three-story moment-resisting frames, with different column-to-beam strength ratios. The results indicate that FRP strengthening is more efficient in frames with a low ratio of column-to-beam strength, due to the type of lateral failure mechanism of the frame. Also, high values of the column-to-beam strength ratio can be benefited by low values of the confining pressure. In case of a column strength greater than a beam strength, beyond a certain confining pressure ratio, further enhancement in performance will not be achieved. Therefore, the level of effective wrapping on frame performance enhancement is controlled by the column-to-beam strength ratio.

INTRODUCTION

Earthquakes in populated regions throughout the world create extensive damage to built-up environments that results in catastrophic human and economical losses. In particular, some Reinforced Concrete (RC) moment-resisting frame systems do not satisfy the desired performance objectives under earthquake excitations. This unacceptable performance can be attributed, in part, to the following. Inadequate design for lateral loading, according to the seismicity of the region, or, from smaller ground motion intensities in previous codes; lack of anticipated member ductility that was either inherent or enforced in the design process; soft soil amplifications and liquefaction in sandy soils and design and construction errors. Moment-resisting frame systems are often desirable in building applications because they allow for maximum floor space utilization and access between bays, especially on the first story of the building, for automobile parking and pedestrian walkways. So, architects prefer this lateral load resisting system, in comparison with systems like shear walls or braced frames.

One of the most important deficiencies of RC frames on seismic attacks is lack of ductility. Causes that significantly reduce member and frame ductility can be summarized as follows; precedence of shear failure, with respect to flexural failure; unsuitable location and length of the longitudinal reinforcement splice; lack of transverse ties or spirals in plastic hinge areas; incorrect location of the rebar cut and improper geometries, which localize the formation of plastic hinges and failure to limited members.

The strength ratio of column-to-beam at connections is the most efficient parameter in directing plastic behavior to specified members. The decrease in this ratio increases the possible formation of plastic hinges in columns, thereby, the energy absorption capability may reduce and, consequently, collapse under gravity load initiates [1]. For providing the desired frame ductility, the ductility demand in a column is much higher in a column mechanism than in a beam mechanism [2].

In recent years, external confinement by the wrapping of FRP sheets (or FRP jacketing) has provided an effective method in enhancing the ductility of existing RC members, especially in columns of structures, such as bridge piers and multistory parking structures [3].

*. *Corresponding Author, Department of Civil Engineering, Sharif University of Technology, Tehran, I.R. Iran.*

1. *Department of Civil Engineering, Sharif University of Technology, Tehran, I.R. Iran.*

This method does not enhance column moment capacity and stiffness significantly. Therefore, additional earthquake forces in the column will not develop, as compared to steel and concrete jacketing, which provides considerable additional stiffness. The FRP wrapping is best used when enhancement in ductility is desired [4].

OBJECTIVE

In strengthening the design of a column with FRP wrapping, adequate attention should be given to the strength ratio of column-to-beam, due to the lesser ductility demand in columns at high values of the column-to-beam strength ratio. Therefore, there has to be a limit in utilizing the FRP strengthening approach, especially when this ratio is relatively high. The objective of this paper is to study the seismic performance of RC frames strengthened with the FRP wrapping of columns, using different column-to-beam strength ratios. Based on the analysis, the influence of this ratio on the effective strengthening will be determined. Moreover, evaluation of the level of improvement in ductility for high column-to-beam strength ratios will be investigated.

METHODOLOGY

The behavior of cylindrical and cubic FRP wrapped concrete specimens was mainly investigated in the 1980s [5]. The purpose of these experiments was to study the effects of FRP confining pressure on the strength and ultimate strain capacity of concrete. On the other hand, some full-scale FRP wrapped columns were tested by studying their ductility capacity. The results indicated that an increase in confining pressure considerably improves the ductility of the member [4].

Moment-Curvature Analysis

In the present study, a stress-strain model, developed previously and based on extensive test results, was selected for Carbon Fiber-Reinforced Plastic (CFRP) confined concrete. Then, a computer code was written to perform moment-curvature analyses, which considers variables such as axial force, longitudinal reinforcement ratio and ratio of confining pressure to unconfined concrete strength. The results of the analysis (ultimate and yielding strength and relevant curvatures) are normalized and arranged in tables to extend their use for general cases. In order to control their generalization ability, all of the analyses were performed on two different section sizes. The results show that normalized parameters are reliable.

Frame Analyses

Following an element behavior investigation, two basic 2D RC moment resisting frames were studied to evaluate the effect of FRP strengthening of a column on the seismic performance of frames. The first frame is a one-story structure, which simulates bridge piers. The second frame is a three-story building, which represents the usual multi-story building structures. In each frame, an initial design was performed to estimate the beam size, using earthquake forces that would be representative of those in a hazardous seismic zone. Next, the flexural strength of the column in the building was varied, based upon the desired column-to-beam strength ratio at the frame joints and the computed beam strength. These considered strength ratios were those that have direct relevance to building in the built-up environment (0.45 to 1.5). For both frames, the beam dimensions and reinforcement were held constant for all column-to-beam strength ratios, which will be introduced later.

The column-to-beam strength ratio was varied by varying the column strength in one of two ways: 1) Holding the gross column diameter constant and changing the steel (that is, constant column stiffness and varied reinforcement ratio) and 2) Varying the column's overall size while maintaining the reinforcement ratio (that is, varied column stiffness and constant reinforcement ratio). Note that, holding the column stiffness constant was the same as holding the column-to-beam stiffness constant for all strength ratios, when reinforcement was neglected in stiffness calculations. Both methods were investigated, so as to isolate the effect of increasing only the column-to-beam strength ratio versus a variation of both strength and stiffness ratios simultaneously.

This yielded four sets of results; 1) A one-story frame (bridge pier), with constant column-to-beam stiffness ratio; 2) A one-story frame (bridge pier) with varied column-to-beam stiffness ratio; 3) A three-story frame, with constant column-to-beam stiffness ratio and 4) A three-story frame, with varied column-to-beam stiffness ratio. Each set of results includes six different models, where each model presents a different column-to-beam strength ratio. Then, each frame was analyzed in the four levels of column strengthening, using a pushover method. Results of the analysis were obtained as lateral strength and ultimate drift enhancement for each frame, with respect to the reference frame with no strengthening.

FRP-CONFINED CONCRETE MODEL

In most applications, the lateral confinement provided by the FRP jacket is passive in nature. When the concrete is subject to axial compression, it expands

laterally. This expansion is confined by the FRP jacket, which is loaded in tension in the hoop direction. As opposed to steel confined concrete, in which the lateral confining pressure is constant following the yielding of steel, the confining pressure provided by the FRP wrap increases with the lateral strain of concrete, because FRP does not yield [6]. The confining action in FRP confined concrete is schematically illustrated in Figure 1, where the f_{frp} and t_{frp} are the stress and thickness of the FRP wrap, respectively.

Lam & Teng [6] proposed an experiment-oriented design-oriented stress-strain relationship, based on the best curve fitting in a wide range of experimental results. Values of the ultimate compressive strain and stress (ε_{cc}, f'_{cc}) for CFRP-confined concrete are expressed by the following two equations, in relation to the unconfined concrete ultimate strain and stress (ε_{co}, f'_{co}). Equation 2 was obtained from regression on only CFRP-confined specimen data.

$$\frac{f'_{cc}}{f'_{co}} = 1.0 + 3.14\frac{f_a}{f'_{co}}, \tag{1}$$

$$\frac{\varepsilon_{cc}}{\varepsilon_{co}} = 1.92 + 24.45\frac{f_a}{f'_{co}}, \tag{2}$$

where actual confining pressure (f_a) is given by:

$$f_a = \frac{2E_{frp}nt\varepsilon_{rup}}{d}, \tag{3}$$

where n, t, d, ε_{rup} and E_{frp} are the number of layers, the thickness of each layer, column diameter, FRP rupture strain and the FRP modulus of elasticity, respectively. The f_a for FRP wraps is about 0.632 of $f_l = 2ntf_{frp}/d$, where f_{frp} is the nominal FRP ultimate tensile strength [6]. The proposed stress-strain model for FRP-confined concrete is given by the following expressions:

For the first parabolic portion ($0 \le \varepsilon_c \le \varepsilon_t$):

$$f_c = E_{co}\varepsilon_c \quad \frac{(E_{co} \quad E_2)^2}{4f'_{co}}\varepsilon_c^2. \tag{4}$$

For the second linear portion ($\varepsilon_t \le \varepsilon_c \le \varepsilon_{cc}$):

$$f_c = f'_{co} + E_2\varepsilon_c. \tag{5}$$

The parabolic first portion meets the linear second portion with a smooth transition at ε_t, which is given by (Figure 2):

$$\varepsilon_t = \frac{2f'_{co}}{(E_{co} \quad E_2)}. \tag{6}$$

where E_2 is the slope of the linear second portion, given by the following equation:

$$E_2 = \frac{f'_{cc} \quad f'_{co}}{\varepsilon_{cc}}. \tag{7}$$

Figure 2 displays the schematic Lam & Teng stress-strain model for FRP-confined concrete [6]. CFRP-confined concrete stress-strain curves for different values of f_l/f'_{co} are drawn in Figure 3 for $f'_{co} = 24.5$ MPa and $\varepsilon_{co} = 0.002$, which are the assumed unconfined concrete strength and relevant strain in the analysis.

MOMENT-CURVATURE ANALYSIS

Material behavior was extended to predict member behavior, using a moment-curvature analysis for a typical circular column cross section, as shown in Figure 4 with $d = 400$ mm and 600 mm. A fiber section model is used for the moment-curvature analysis. Section mesh is optimized using sensitivity analysis on different meshing forms. The outer fiber size is reduced, due to its significant effect on the accuracy of the results,

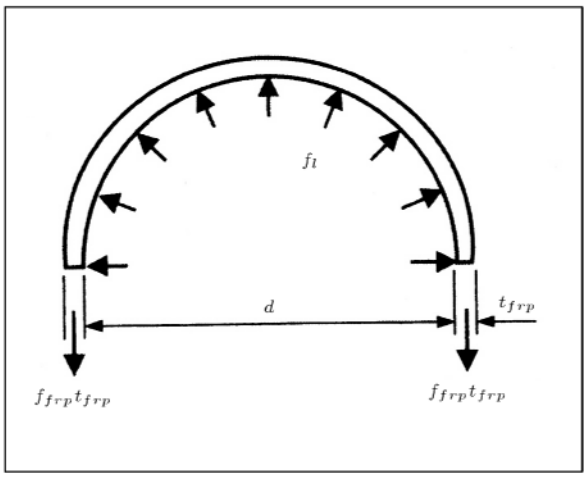

Figure 1. Confining action.

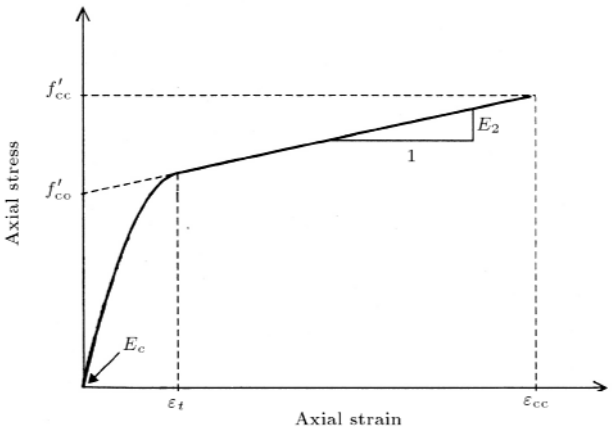

Figure 2. Schematic FRP confined concrete stress-strain model (Lam and Teng [6]).

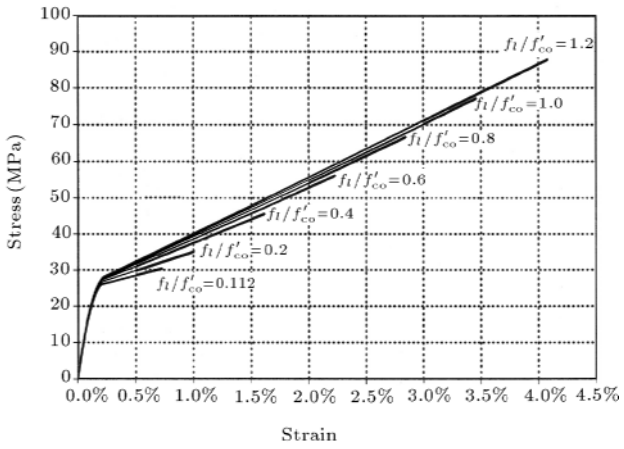

Figure 3. CFRP-confined concrete stress-strain curves with different confining ratio for $f'_{co} = 24.5$ MPa.

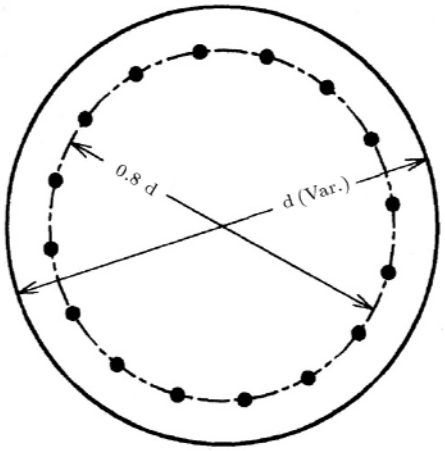

Figure 4. Typical column section.

especially at ultimate curvatures. The number of circumferential segments is increased at a greater distance from the center. Figure 5a displays common polar meshing and Figure 5b displays the typical section meshing used in moment-curvature analysis, in which the number of circumferential segments is doubled in three steps.

Table 1 presents the sensitivity analysis result, which compares the error of each mesh formation with

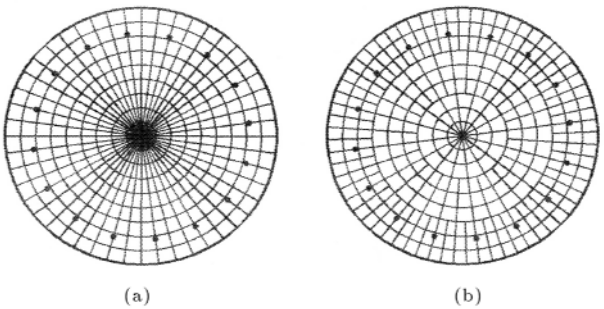

Figure 5. (a) Common polar mesh; (b) refined mesh.

Table 1. Sensitivity analyses results on mesh formation.

Section Designation	No. of Elements	Error in f_u (%)	Error in M_u(%)
G12C6	162	10.42	0.86
G12C12	324	6.50	0.73
G12C18	486	5.44	0.67
G21C6	270	6.80	0.51
G21C12	540	3.02	0.34
G21C18	810	2.11	0.26
G30C6	378	5.44	0.33
G30C12	756	1.81	0.18
G30C18	1134	0.76	0.09
G39C30	2430	-	-

a very fine mesh formation (G39C30) in predicting the values of the ultimate moment strength and ultimate curvature. Symbol G represents the number of radial segments and C represents the number of circumferential segments at the center. Based on these results, due to the sufficient accuracy of the meshing form of G21C12, this meshing form is selected for all subsequent moment-curvature analyses.

The column sections were analyzed at unconfined and at ten levels of the confining ratio (i.e., f_l/f'_{co} assumed $0.112, 0.2, 0.4, \cdots, 1.2$) under axial forces, which varied from zero to $1.0f'_{co}A_g$, where each set has reinforcement ratios ranging from 1% to 7%. Sections in the unconfined condition (before strengthening) were analyzed using the Mander et al. unconfined concrete model [7]. The analytical representation of the stress-strain curve of steel with a yield plateau and strain-hardening portion, proposed by Wang, Shah and Naaman [8] and based on numerous experimental results, is utilized for longitudinal steels. The yielding and ultimate stress of the steel were assumed to be 400 MPa, and 600 MPa, respectively. Figures 6 and 7 present typical interaction curves obtained from a moment-curvature analysis. The effect of CFRP-confining pressure on ultimate flexural capacity increases by increasing the axial load. At low values of axial force, the moment capacity enhancement, due to CFRP confinement, is not significant (Figures 6a and 6b). Ductility enhancement, at low values of axial force, is much higher than at high axial loads (Figures 7a and 7b). The moment-curvature curves approximated by bilinear form and values of M_y, M_u, φ_y and φ_u are calculated for the frame analysis.

SELECTED FRAMES

Figures 8 and 9 show the geometries of frames selected, as introduced earlier. The distributed gravity loads on

Table 2. Beam details of one and three story frames.

Location	Reinforcement (cm^2)		Moment Capacity (kN.m)	
	Top	Bottom	Yielding	Ultimate
One-Story ($h = 120$ cm, $b = 150$ cm)				
Middle beams	60	60	3015.6	3289.3
Edge beams	120	120	4944.2	6722.8
Three-Story ($h = 40$ cm, $b = 35$ cm)				
Middle roof beams	12	12	191.3	194
Roof edge beams	25	25	388.5	397.3
Middle story beams	25	25	388.5	397.3
Edge story beams	50	50	758.3	788

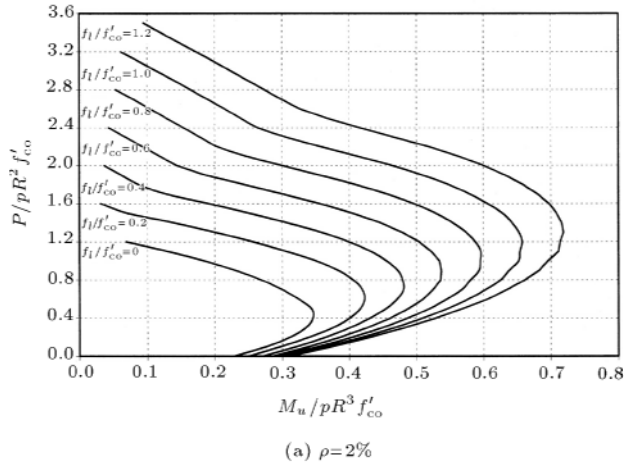

(a) ρ=2%

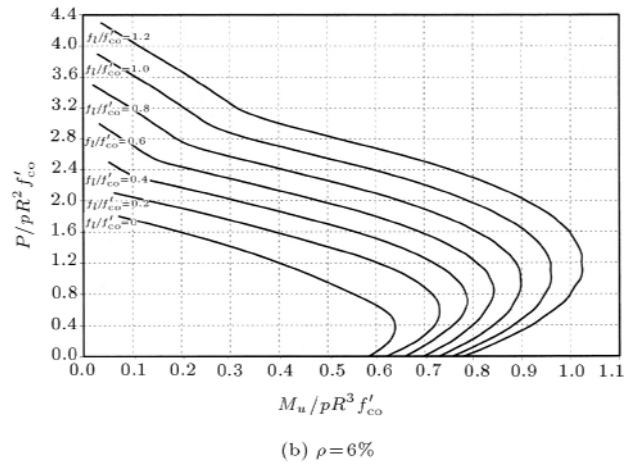

(b) ρ=6%

Figure 6. Typical moment capacity-axial force interaction curves.

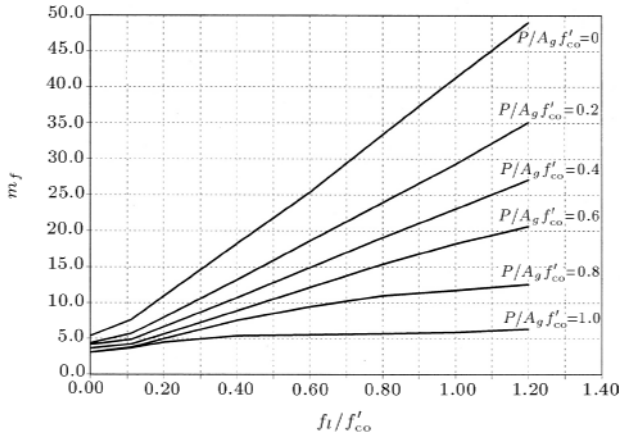

(a) ρ=2%

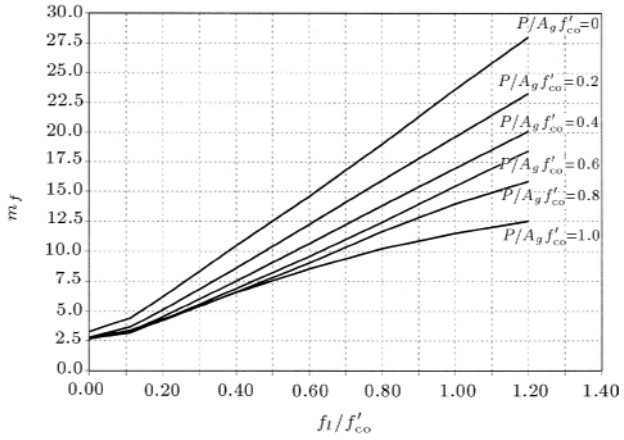

(b) ρ=6%

Figure 7. Typical ductility-confining pressure ratio interaction curves.

the beams of one-story and three-story frames were 490.5 kN/m and 34.3 kN/m, respectively. Table 2 introduces beam sections and reinforcement. Edge beams are twice as strong as middle beams, in order to maintain the column-to-beam strength ratio as constant at all joints. Also, the moment strength of roof beams is one-half of the beams in lower stories. Variations of the column-to-beam strength ratio and column details are given in Tables 3 and 4. The reinforcement ratio has changed from 1 to 6 percent,

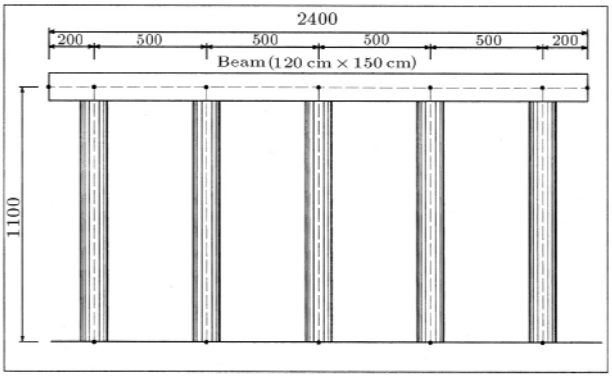

Figure 8. One-story frame geometry (bridge pier).

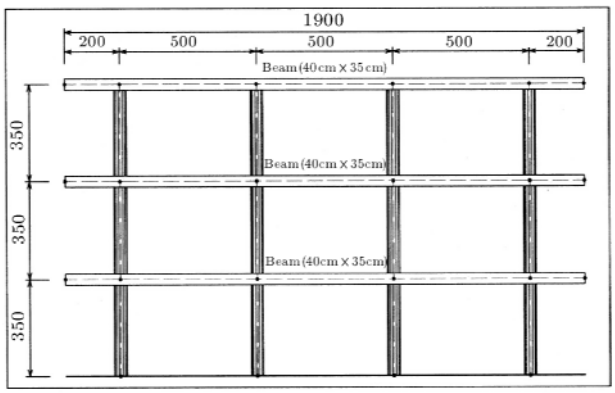

Figure 9. Three-story frame geometry.

while the column dimension is kept constant (6 cases for constant stiffness). Moreover, the reinforcement ratio is kept constant, while the column diameter is determined, based on the similar column-to-beam strength ratio of the first 6 cases (6 cases for varied stiffness). The initial design of the column resulted in $\rho = 2.0\%$ and $d = 120$ cm in a one-story frame and $\rho = 3.0\%$ and $d = 45$ cm in a three-story frame.

PUSH-OVER ANALYSIS AND RESULTS

The plastic behavior of each element is concentrated in plastic hinges located at the two ends of the beams and columns. In order to allow for the shifting of the plastic hinge location in beams, due to gravity loads, two plastic hinges were introduced at each end of the beams with a distance of one tenth of the beam length. The plastic hinge length was considered as three-fourths of the beam depth or column diameter for beams and columns, respectively. The remaining element's length was assumed to be elastic (i.e., a lumped plasticity model was used). Interaction of the axial force-flexural capacity and the axial force-ductility of the columns was obtained from a moment-curvature analysis (Figures 6 and 7). A bilinear moment-curvature, as an element plastic behavior characteristic, is introduced to the program. Shear deformations and shear failure are not included in the analysis.

The pushover analysis of the frames is performed by PERFORM2D-3.10, educational version. The lateral force was exerted by a triangular load pattern. The frames are pushed until one of the plastic hinges reaches ultimate curvature. The displacement was monitored at roof level. The pushover curves obtained from the analyses are presented in terms of base shear versus roof drift. Results were summarized as ultimate drift and maximum base shear enhancement, in comparison to frames without column strengthening.

Figures 10a, b and c display typical base shear-roof drift curves for different column-to-beam strength ratios in a one-story frame. It is observed that, by increasing the column-to-beam strength ratio, the effectiveness of the column FRP jacketing decreases considerably. By increasing the confining ratio, enhancement in the frame ductility was no longer significant (Figure 10c). Figures 11 to 14 show the enhancement percentage in the roof drift and ultimate base-shear (strength) of the frames. Figures 11 and

Table 3. One-story column details and column-to-beam strength ratio.

Section Designation	ρ (%)	d (cm)	M_u (kN.m)	$\Sigma M_c/\Sigma M_b$
PC11	1.0	120.0	3034	0.46
PC12	2.0	120.0	4571	0.69
PC13	3.0	120.0	6013	0.91
PC14	4.0	120.0	7427	1.13
PC15	5.0	120.0	8788	1.34
PC16	6.0	120.0	10134	1.54
PC21	2.0	102.5	2992	0.45
PC22	2.0	120.0	4571	0.69
PC23	2.0	132.5	5977	0.91
PC24	2.0	142.5	7299	1.11
PC25	2.0	152.5	8808	1.34
PC26	2.0	160.0	10071	1.53

Table 4. Three-story column details and column-to-beam strength ratio.

Section Designation	ρ (%)	d (cm)	M_u (kN.m)	$\Sigma M_c/\Sigma M_b$
FC11	1.0	45.0	180.7	0.45
FC12	2.0	45.0	257.1	0.65
FC13	3.0	45.0	330.4	0.83
FC14	4.0	45.0	401.9	1.01
FC15	5.0	45.0	472.7	1.19
FC16	6.0	45.0	542.0	1.36
FC21	3.0	36.2	180.8	0.46
FC22	3.0	41.5	263.9	0.66
FC23	3.0	45.0	440.4	0.83
FC24	3.0	48.1	398.0	1.00
FC25	3.0	51.3	476.1	1.20
FC26	3.0	53.9	546.5	1.38

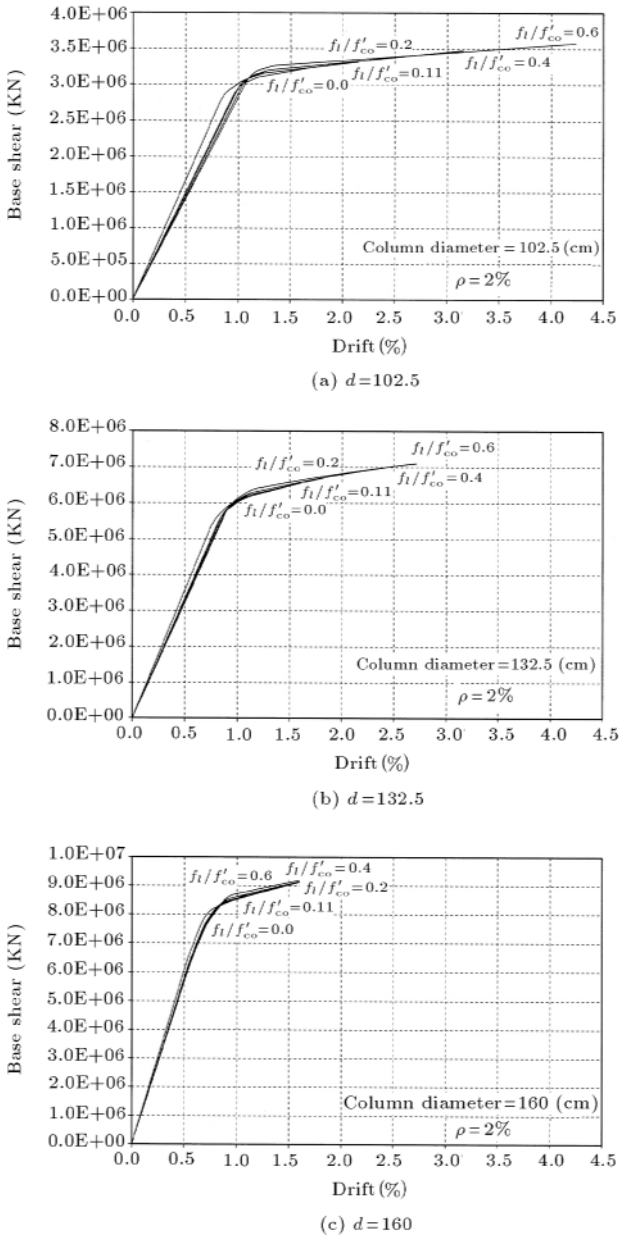

Figure 10. Typical push-over results of one-story frame.

12 contain four graphs related to a single story frame (bridge pier) and Figures 13 and 14 contain four graphs pertaining to a three-story frame. Each group has two subgroups, according to the method of column-to-beam strength ratio variation (constant stiffness or varied stiffness). Results showed that, by increasing the column-to-beam strength ratio, the percentage of enhancement in the performance of the frame (ultimate drift and maximum base shear) decreases at high values of f_l/f'_{co}. However, at low values of the confining pressure ratio, the higher column-to-beam strength ratios experience a higher increase in frame strength (this strength enhancement is limited to 17.5% for a three-story frame and 9.0% for a one-story frame) (Figures 12 and 14).

If column-to-beam strength ratio exceeds a value of about one, the enhancement takes place up to a certain confining pressure and a further increase in confining pressure no longer enhances the behavior. In other words, at a column-to-beam ratio of about one, the curves become flat at a certain confining pressure ratio. The level of enhancement in ultimate drift can reach up to 300 percent, depending on the column-to-beam strength ratio; however, the ultimate base shear (strength) enhancement is limited to 30 percent. The above conclusion can be extended, also, to the three-story frame, confirming the generality of the results.

SUMMARY AND CONCLUSIONS

Based on the moment-curvature analysis, the FRP confinement system enhances the ductility of the column; however, it does not significantly improve flexural strength. An increase in confining pressure increases the ductility, especially at low values of the axial load and longitudinal reinforcement ratio.

The column-to-beam strength ratio, as an important parameter in strengthening the design of a frame using the FRP jacketing of columns, was studied. A push-over analysis of a 2D model was performed on one

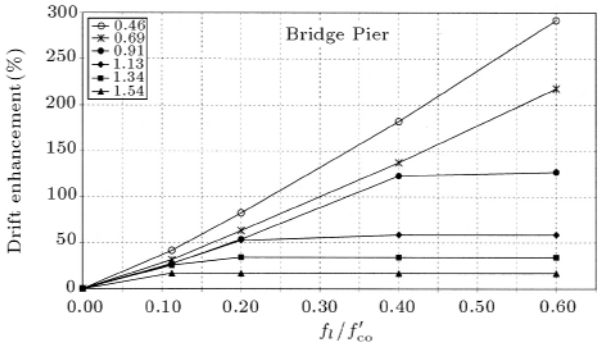

(a) Constant stiffness

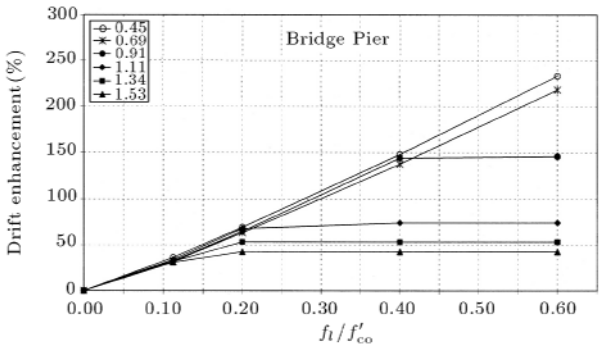

(b) Varied stiffness

Figure 11. Drift enhancement percentage for one-story frame.

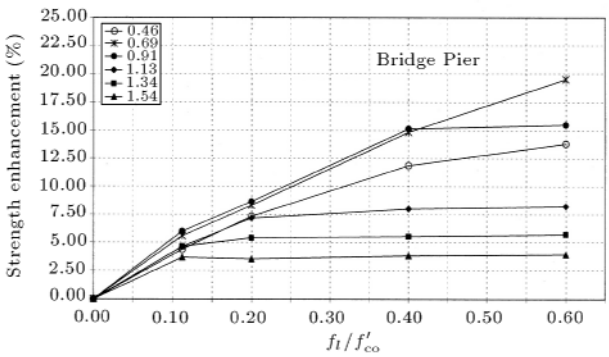

(a) Constant stiffness

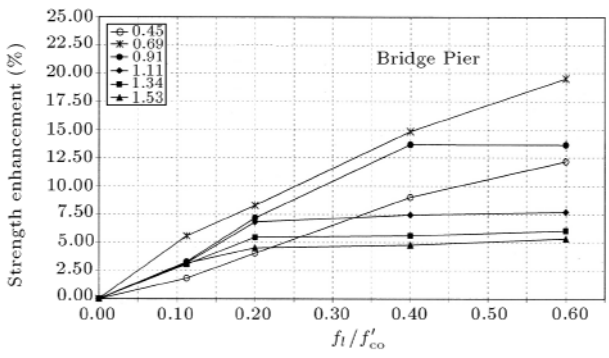

(b) Varied stiffness

Figure 12. Strength enhancement percentage for one-story frame.

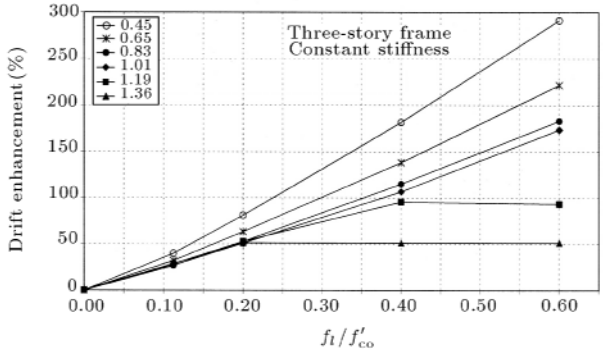

(a) Constant stiffness

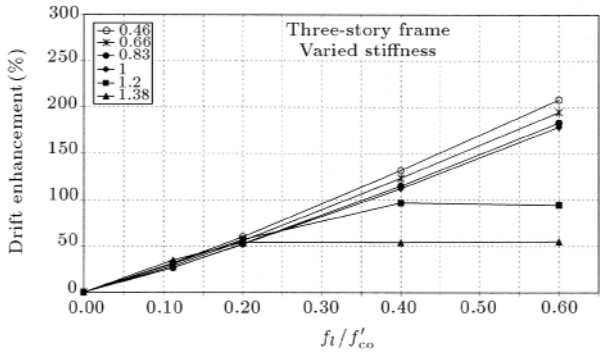

(b) Varied stiffness

Figure 13. Drift enhancement percentage for three-story frame.

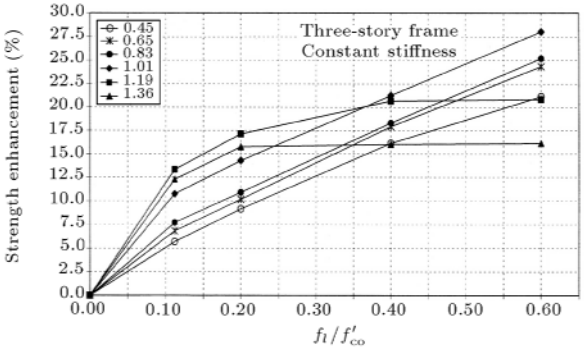

(a) Constant stiffness

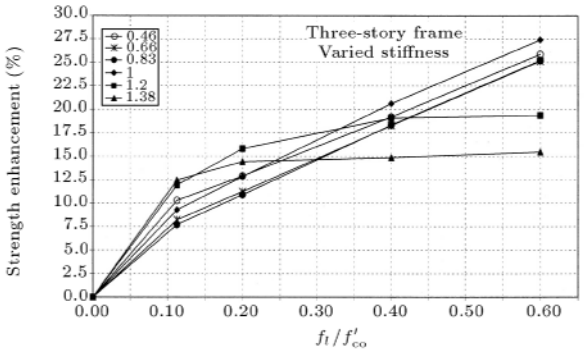

(b) Varied stiffness

Figure 14. Strength enhancement percentage for three-story frame.

and three-story moment-resisting frames with different column-to-beam strength ratios. The results indicate that FRP strengthening is more efficient in frames with a low ratio of column-to-beam strength, due to the type of lateral failure mechanism of the frame. High values of the column-to-beam strength ratio can be benefited from low values of confining pressure. If the column-to-beam strength ratio exceeds a value of about one, the enhancement takes place up to a certain confining pressure and a further increase in confining pressure does not further enhance the frame performance. The primary benefit of the FRP wrapping of columns is the improvement in the deformation capacity (ductility) of the frame, where strength enhancement is of a second order. The conclusions can also be extended to a three-story frame, confirming the generality of the results.

A comparison of the results, based on the two methods of varying column-to-beam strength ratios (i.e., constant and varied stiffness), indicated that if the low value of this ratio were due to a low value of column reinforcement (constant stiffness), CFRP jacketing would be more efficient in increasing frame ductility than the low value of the column-to-beam strength ratio, due to the small diameter of the column (varied stiffness).

ACKNOWLEDGMENT

The authors appreciate the support provided by the Research Committee of Sharif University of Technology in conducting this research study.

REFERENCES

1. Kara, L.D. and Bracci, J.M. "Seismic evaluation of column-to-beam strength ratio in reinforced concrete frames", *ACI Structural Journal*, **98**(6), pp 843-851 (2001).
2. Park, R. and Paulay, T., *Reinforced Concrete Design*, New York, John Wiley and Sons (1975).
3. Van Den Einde, L., Zhao, L. and Seibel, F. "Use of FRP in civil structure applications", *J. Construction and Building Material*, **17**, pp 389-403 (2003).
4. Teng, G.J., Chen, J.F., Smith, S.T. and Lam, L., *FRP Strengthened RC Structures*, England, John Wiley and Sons (2001).
5. De Lorenzis, L. and Tepfers, R., *A Comparative Study of Model on Confinement of Concrete Cylinder with FRP Composite*, Publication No: 01:46, Dept. of Building Materials, Chalmers University of Technology, Sweden (2001).
6. Lam, L. and Teng, J.G. "Design-oriented stress-strain model for FRP-confined concrete", *Journal of Construction and Building Materials*, **17**, pp 471-489 (2003).
7. Mander, J.B., Priestley, M.J.N. and Park, R. "Theoretical stress-strain model for confined concrete", *Journal of Structural Engineering, ASCE*, **114**(8), pp 1804-1826 (1988).
8. Wang, P.I., Shah, S.P. and Naaman, A.E. "High-strength concrete in strength design", *J. Structural Division, ASCE*, **104**, pp 1761-1773 (1978).